Inorg. Chem. **2005**, *44*, 4719–4727

The Reactions of Nitrosyl Complexes with Cysteine

Federico Roncaroli and José A. Olabe*

Departamento de Química Inorgánica, Analítica y Química Física—INQUIMAE, Facultad de Ciencias Exactas y Naturales, Universidad de Buenos Aires—CONICET, Pabellón 2, Ciudad Universitaria, Buenos Aires C1428EHA, Argentina

Received December 30, 2004

The reaction kinetics of a set of ruthenium nitrosyl complexes, $\{(X)_5MNO\}^n$, containing different coligands X (polypyridines, NH_3, EDTA, pz, and py) with cysteine (excess conditions), were studied by UV–vis spectrophotometry, using stopped-flow techniques, at an appropriate pH, in the range 3–10, and $T = 25$ °C. The selection of coligands afforded a redox-potential range from –0.3 to +0.5 V (vs Ag/AgCl) for the NO^+/NO bound couples. Two intermediates were detected. The first one, $\mathbf{I_1}$, appears in the range 410–470 nm for the different complexes and is proposed to be a 1:1 adduct, with the S atom of the cysteinate nucleophile bound to the N atom of nitrosyl. The adduct formation step of $\mathbf{I_1}$ is an equilibrium, and the kinetic rate constants for the formation and dissociation of the corresponding adducts were determined by studying the cysteine-concentration dependence of the formation rates. The second intermediate, $\mathbf{I_2}$, was detected through the decay of $\mathbf{I_1}$, with a maximum absorbance at ca. 380 nm. From similar kinetic results and analyses, we propose that a second cysteinate adds to $\mathbf{I_1}$ to form $\mathbf{I_2}$. By plotting ln $k_{1(RS^-)}$ and ln $k_{2(RS^-)}$ for the first and second adduct formation steps, respectively, against the redox potentials of the NO^+/NO couples, linear free energy plots are obtained, as previously observed with OH^- as a nucleophile. The addition rates for both processes increase with the nitrosyl redox potentials, and this reflects a more positive charge at the electrophilic N atom. In a third step, the $\mathbf{I_2}$ adducts decay to form the corresponding Ru–aqua complexes, with the release of N_2O and formation of cystine, implying a two-electron process for the overall nitrosyl reduction. This is in contrast with the behavior of nitroprusside ($[Fe(CN)_5NO]^{2-}$; NP), which always yields the one-electron reduction product, $[Fe(CN)_5NO]^{3-}$, either under substoichiometric or in excess-cysteine conditions.

Introduction

The reactivity of nitrogen monoxide (NO) bound to transition metal centers is of particular concern in the context of the chemistry of NO relevant to biology.[1] When discussing the ability of NO to bind or dissociate from a given metal, it is crucial to define the redox state of the nitrosyl-bound species. The redox interconversions in the MNO moieties can lead to species with different electron contents, which may be described, in limiting approximations, as $M(NO^+)$, M(NO), or $M(NO^-)$. The electronic structures can be discussed with the aid of spectroscopic tools (mainly IR and EPR) or theoretical calculations, corresponding, in each case, to different reactivity patterns for the formation/dissociation rates, as well as for other types of redox reactivity.[2] The nitroprusside ion (NP; $[Fe(CN)_5NO]^{2-}$) is unique among iron—nitrosyl complexes with biological activity.[3] In addition to its hypotensive action, other physiological roles have been described in a recent review.[4] The long-known reversible additions of nucleophiles have been studied with NP and other metallonitrosyls by using OH^-, amines, thiolates, and other reactants.[5] In these reactions, the electrophilic nitrosyl ligand can be best described as a nitrosonium (NO^+) species, with the N atom being the site for the addition of the nucleophiles.[3,5]

The mechanistic study of the reaction of NP with OH^- has been extended recently to a great variety of nitrosyl

* Author to whom correspondence should be addressed. E-mail: olabe@qi.fcen.uba.ar.

(1) (a) McCleverty, J. A. *Chem. Rev.* **2004**, *104*, 403−418. (b) Stamler, J. S.; Feelisch, M. In *Methods in Nitric Oxide Research*; Feelisch, M., Stamler, J. S., Eds.; Wiley: Chichester, U. K., 1996; Chapter 2. (c) *Nitric Oxide: Biology and Pathobiology*; Ignarro, L. J., Ed.; Academic Press: San Diego, CA, 2000. (d) Moncada, S.; Palmer, R. M. J.; Higgs, E. A. *Pharmacol. Rev.* **1991**, *43*, 109−142.

(2) (a) Westcott, B. L.; Enemark, J. H. In *Inorganic Electronic Structure and Spectroscopy*; Solomon, E. I., Lever, A. B. P., Eds.; Wiley Interscience: New York, 1999; Vol. 2, Chapter 7, pp 403−450. (b) Enemark, J. H.; Feltham, R. D. *Coord. Chem. Rev.* **1974**, *13*, 339−406.

(3) (a) Swinehart, J. H. *Coord. Chem. Rev.* **1967**, *2*, 385−402. (b) Clarke, M. J.; Gaul, J. B. *Struct. Bonding (Berlin)* **1993**, *81*, 147−181. (c) Butler, A. R.; Glidewell, C. *Chem. Soc. Rev.* **1987**, *16*, 361−380.

(4) Butler, A. R.; Megson, I. L. *Chem. Rev.* **2002**, *102*, 1155−1165.

10.1021/ic048156d CCC: $30.25
Published on Web 05/20/2005

complexes of formula type $\{(X)_5MNO\}^n$, with X comprising ligands of different donor−acceptor abilities, such as amines, polypyridines, cyanides, and so forth.[5,6] Most of these studies have been performed with ruthenium, but a similar picture emerges with other low-spin d^6 metals such as Fe(II), Os(II), and Ir(III). The reactions with OH^- are mechanistically simple; they can be considered as acid−base reactions evolving in two steps: first, OH^- is added, forming the $\{(X)_5MN(O)OH\}$ intermediate, which may go back to $M(NO^+)$ or subsequently lose the proton rapidly under the attack of another OH^- to give the final nitro complex. In the previous work,[6] the redox potentials of the $M(NO^+)/M(NO)$ couples were shown to be the crucial factors controlling the electrophilic reactivity of the different $\{(X)_5MNO\}^n$ complexes.

The reactions with other potentially reductant nucleophiles such as amines or thiolates are more complicated than those with OH^-, because irreversible processes (namely, intramolecular redox reactions) operate subsequently to adduct formation. The reactions with N-binding nucleophiles (ammonia and amines, hydrazine, hydroxylamine, and azide) binding to different metal centers have been reviewed,[5,7] and they lead to gas evolution (N_2 or N_2O) as a result of the adduct decompositions, with complex mechanistic issues that are dependent on the structure of the metallonitrosyl−nucleophile adducts. On the other hand, the reactions of different thiolates have been addressed exclusively with NP.[8−10] Adduct intermediates intensively absorbing around 520 nm have been observed for the fast reactions of NP with diverse thiolates,[8,9] with ensuing decomposition processes involving the reduction of NO^+ and the oxidation of the thiolates.[10] Remarkably, one- or two-electron reduction products have been detected in different circumstances with NP. Either in substoichiometric or in excess conditions of thiolate, the $[Fe(CN)_5NO]^{3-}$ ion appears as the ultimate main product of thiolate additions to NP, in the pH range 8−10 (cyanide release forming predominantly $[Fe(CN)_4NO]^{2-}$ occurs at lower pHs). This has been found for cysteine, glutathione, and other thiolates.[10a,b] At pH 6−8, free NO has been claimed to be released from $[Fe(CN)_4NO]$,$^{2-}$ [10c,d] and even bound NO^- (nitroxyl) has been reported as an intermediate in the NP−cysteine reaction.[10d] The mode of nitroxyl generation and characterization remains obscure, however (e.g., no N_2O has been detected). To complete this intriguing picture, N_2O has been detected by IR during the reaction of NP with excess glutathione and other reductants at pH 7.2.[10e]

In a very recent work, the $[Fe(CN)_5NO]^{3-}/[Fe(CN)_4NO]^{2-}$ complexes (generated by controlled reduction of NP using dithionite or tetrahydroborate, pH range 4−10) were *both* shown to release NO very slowly ($k = \sim 10^{-5}$ s^{-1}). The fate of free NO was related to the further formation of dinitrosyls, followed by a disproportionarion process leading to N_2O and the regeneration of NP.[11a] Among the final products, EPR-active compounds have been also found, related to those of formula type $\{Fe(NO)_2L_2\}$ (L = thiolates, imidazole, etc.), referred to as "g = 2.03" complexes. These have been previously suggested to be direct precursors of sGC activation.[11b] Evidently, all of these reactions are of great biological relevance, because NP is currently injected into the bodily fluids for blood-pressure control, and the question arises on the eventual mechanistic role of thiolates in the mobilization of NO, in order for it to be accessible in solution for the vasodilation process.[3,4] In this report, we refer to the latter issue only as a final comment, because our main goal is to introduce a broader picture for the reactivity studies of thiols with metal nitrosyls, in addition to the work published for the NP ion. This has revealed a complex mechanism, involving nonradical and radical paths, as well as a significant influence of pH and oxygen availability on the reaction process.[10a] We have selected cysteine $\{H_3N^+CH(CO_2^-)CH_2SH\}$ as the starting reagent for S-nucleophilic binding, because of the biological relevance, and we use a variety of ruthenium nitrosyl complexes already well-characterized in the literature.[12] We focus on the stoichiometry and mechanism of the processes arising after mixing the nitrosyl complexes with an excess of cysteine under anaerobic and pH-controlled conditions, and we address the conditions favoring the one- or two-electron reduction of bound NO^+, aiming at the comparison with previous results in the reactions of NP with the thiolates.

Experimental Section

Materials and Methods. All chemicals were analytical grade and were used without further purification. L-Cysteine hydrochloride monohydrate was purchased from Anedra. Sodium nitroprusside dihydrate (NP) was from Aldrich. The following ruthenium complexes were prepared as described in the literature: $[Ru(bpz)NO(tpy)](PF_6)_3$,[12a] *cis*-$[Ru(AcN)(bpy)_2NO](PF_6)_2$,[12b] *cis*-$[Ru(bpy)_2(NO_2)NO](PF_6)_2$,[12c] *cis*-$[Ru(bpy)_2ClNO](PF_6)_2$,[12c] $[Ru(bpy)NO(tpy)](PF_6)_3$,[12d] *trans*-$[Ru(NH_3)_4NO(pz)](BF_4)_3$,[12e] [Ru(HEDTA)NO],[12f]

(5) (a) Bottomley, F. In *Reactions of Coordinated Ligands*; Braterman, P. S., Ed.; Plenum Press: New York, 1989; Vol. 2, pp 115−222. (b) Ford, P. C.; Lorkovic, I. M. *Chem. Rev.* **2002**, *102*, 993−1018. (c) Ford, P. C.; Laverman, L. E.; Lorkovic, I. M. *Adv. Inorg. Chem.* **2003**, *54*, 203−257.

(6) Roncaroli, F.; Ruggiero, M. E.; Franco, D. W.; Estiú, G. L.; Olabe, J. A. *Inorg. Chem.* **2002**, *41*, 5760−5769.

(7) Olabe, J. A. *Adv. Inorg. Chem.* **2004**, *55*, 61−126.

(8) Johnson, M.; Wilkins, R. G. *Inorg. Chem.* **1984**, *23*, 231−235.

(9) Szacilowski, K.; Stochel, G.; Stasicka, Z.; Kisch, H. *New J. Chem.* **1997**, *21*, 893−902.

(10) (a) Szacilowski, K.; Wanat, A.; Barbieri, A.; Wasielewska, E.; Witko, M.; Stochel, G.; Stasicka, Z. *New J. Chem.* **2002**, *26*, 1495−1502. (b) Morando, P. J.; Borghi, E. B.; Schteingart, L. M.; Blesa, M. A. *J. Chem. Soc., Dalton Trans.* **1981**, 435−440. (c) Butler, A. R.; Calsy-Harrison, A. M.; Glidewell, C. *Polyhedron*, **1988**, *7*, 1197−1202. (d) Smith, J. N.; Dasgupta, T. P. *Inorg. React. Mech. (Philadelphia, PA, U. S.)* **2002**, *3*, 181−195. (e) Sampath, V.; Rousseau, D. L.; Caughey, W. In *Methods in Nitric Oxide Research*; Feelisch, M., Stamler, J. S., Eds.; Wiley: Chichester, U. K., 1996; Chapter 29.

(11) (a) Roncaroli, F.; van Eldik, R.; Olabe, J. A. *Inorg. Chem.* **2005**, *44*, 2781−2790. (b) Aliev, D. I.; Vanin, A. F. *Russ. J. Phys. Chem.* **1982**, *56* (9), 1452−1455.

(12) (a) Frantz, S.; Sarkar, B.; Sieger, M.; Kaim, W.; Roncaroli, F.; Olabe, J. A.; Zalis, S. *Eur. J. Inorg. Chem.* **2004**, 2902−2907. (b) Callahan, R. W.; Meyer, T. J. *Inorg. Chem.* **1977**, *16*, 574−581. (c) Godwin, J. B.; Meyer, T. J. *Inorg. Chem.* **1971**, *10*, 471−474. (d) Murphy, R. W.; Takeuchi, K.; Barley, M. H.; Meyer, T. J. *Inorg. Chem.* **1985**, *25*, 1043. (e) Gomes, M. G.; Davanzo, C. V.; Silva, S. C.; Lopes, L. G. F.; Santos, P. S.; Franco, D. W. *J. Chem. Soc., Dalton Trans.* **1998**, 601−607. (f) Zanichelli, P. G.; Miotto, A. M.; Estrela, H. G.; Rocha Soares, F.; Grassi-Kassisse, D. M.; Spadari-Bratfisch, R. C.; Castellano, E. E.; Roncaroli, F.; Parise, A. R.; Olabe, J. A.; de Brito, A. R. M. S.; Franco, D. W. *J. Inorg. Biochem.* **2004**, *98*, 1921−1932. (g) Roncaroli, F.; Baraldo, L. M.; Slep, L. D.; Olabe, J. A. *Inorg. Chem.* **2002**, *41*, 1930−1939.

Table 1. UV−Vis Maximum Absorptions (nm) of $\mathbf{I_1}$ and $\mathbf{I_2}$ for Different Nitrosyl Complexes[a]

	complex	intermediate 1		intermediate 2	
1	$[Fe(CN)_5NO]^{2-}$	526	(10^3-10^4)[b]		
2	$[Ru(HEDTA)NO]^-$	405[c]		340[c]	
3	*trans*-$[Ru(NH_3)_4NO(pz)]^{3+}$	421[d]		336[d]	
4	*cis*-$[Ru(bpy)_2ClNO]^{2+}$	450	(8.0×10^3)	384	(5.3×10^3)
		410 (sh)	(6.8×10^3)		
5	*cis*-$[Ru(bpy)_2(NO_2)NO]^{2+}$	451	(7.6×10^3)	372	(6.6×10^3)
		376			
6	*trans*-$[NCRu(py)_4CNRu(py)_4NO]^{3+}$	461		425 (sh)	
7	$[Ru(bpy)NO(tpy)]^{3+}$	467	(9.0×10^3)	394	(6.2×10^3)
		390	(6.0×10^3)		
8	*cis*-$[Ru(AcN)(bpy)_2NO]^{2+}$	448	(3×10^3)	390	
9	$[Ru(bpz)NO(tpy)]^{3+}$	467	(5.6×10^3)		

[a] Values in parentheses correspond to molar absorbances. pH 4.0 (0.1 M acetate buffer), $I = 1$ M (NaCl), $T = 25.0$ °C. At least a 10-fold excess of cysteine over the complex concentration was used, unless otherwise stated. [b] From refs 8 and 9. [c] pH 9.9 (0.1 M borate buffer), $I = 1$ M (NaCl). [d] pH 7.0 (0.1 M phosphate buffer), $I = 1$ M (NaCl).

and *trans*-$[NCRu(py)_4CNRu(py)_4NO](PF_6)_3$[12g] (tpy = terpyridine; bpz = 2,2′-bipyrazine; bpy = 2,2′-bipyridine; pz = pyrazine; py = pyridine). The purities were checked by IR and ^{1}H NMR spectroscopy. Solutions were deoxygenated by saturation with N_2 or Ar. They were protected from light and were handled using gastight syringes. 1 M NaCl was used for adjusting the ionic strength, and acetic, phosphate, and borate buffers were employed to control the pH.

Instrumentation and General Procedures. pH measurements were done with a Metrohm 744 pH meter at room temperature. NMR spectra were recorded on a Brucker 500 MHz spectrometer. A Thermo Nicolet Avatar 320 FT-IR spectrometer and a Spectratech IR liquid cell (with two 32 × 3 mm CaF_2 disks and a 0.1 mm spacer) were used for the IR measurements. Usually, a 10−15 mM solution in *cis*-$[Ru(bpy)_2ClNO]Cl_2$ was prepared in D_2O or H_2O, after saturation with Ar. The necessary amount of cysteine was added together with some sodium acetate or sodium carbonate to reach the desired pH. A 273A Princeton Applied Research Potentiostat was used for square wave voltammetry (SWV) and electrolysis. For SWV, a solution containing 1 M NaCl and 0.1 M sodium acetate at pH 4 was used as an electrolyte. Vitreous carbon, Ag/AgCl (3 M KCl), and a platinum wire were used as working, reference, and counter electrodes, respectively. EPR measurements were done on the X-band of a Brucker ER 200D spectrometer. The spectra were recorded at 9.57 GHz, at 140 K. For these experiments, 1 mM *cis*-$[Ru(bpy)_2ClNO](PF)_6$ solutions were prepared (0.1 M acetate, $I = 1$ M, pH 4.0), and 0.8 mg or 20 mg of cysteine were added to 10 mL of the complex solution, depending upon the experiment. UV−vis spectra were recorded in the range 200−1100 nm with a Hewlett-Packard 8453 diode array spectrophotometer. For the titrations of the complexes with cysteine, 20 mL of a 5×10^{-5} M complex solution (0.1 M acetic buffer; pH 4.0; $I = 1$ M) were placed in a cuvette attached to a flask. After bubbling N_2, 0.1-mL aliquots of a 2×10^{-3} M solution of cysteine were added. The UV−vis spectral changes were recorded during the process as described previously. The titrations were done in duplicates. The temperature was kept constant at 25.0 ± 0.1 °C by means of a Lauda RC 20 thermostat.

Kinetic Experiments. A solution containing the complex (7×10^{-5} to 5×10^{-4} M, depending on the complex and the concentration of cysteine, with 1 M NaCl) and some HCl (pH ∼2 to discard any reaction with OH^-) was mixed using stopped-flow (SF) techniques with another solution containing cysteine (6×10^{-4} to 1.4×10^{-2} M), the buffer system (0.1−0.5 M), and NaCl to reach a total $I = 1$ M. At least a 10-fold excess of cysteine over the concentration of the complex was always kept to ensure pseudo-first-order conditions. To get an overall picture of the reaction, the solutions were mixed using an RX 1000 Applied Photophysics rapid kinetic accessory, and the spectral changes were recorded on the diode array spectrophotometer. To make the systematic studies as a function of the concentration of cysteine or of the pH, a Hi Tech PQ/SF-53 stopped-flow and a Hi Tech SU-40 spectrophotometric unit were used. The data were acquired by a Hewlett-Packard 54600A oscilloscope. This last instrument was interfaced with a computer. The wavelength was always selected close to the absorption maximum of intermediate 1 ($\mathbf{I_1}$) (410−470 nm for the ruthenium complexes and 526 nm for NP, see Table 1). Kinetic traces were always fitted to a single exponential for at least three half-lives, usually five, with the aid of a homemade program. Under each condition, about 10 measurements were done; values that differed less than 20%, usually less than 10%, were averaged. In this way, k_{obs} values were obtained. Plots of k_{obs} versus cysteine concentration afforded the formation second-order rate constant, with an intercept value equal to the dissociation constant (see eq 1). The formation of $\mathbf{I_1}$ could only be studied using the Hi Tech SF technique. Similar values on the decomposition of $\mathbf{I_1}$ (to produce intermediate 2, $\mathbf{I_2}$) were obtained using both groups of instruments. For the experiments as a function of pH, a 9×10^{-5} M solution of $[Ru(bpy)_2ClNO]^{2+}$ and an 8.2×10^{-3} M solution of cysteine were used. The second-order rate constant was calculated from the observed rate constants and the cysteine concentration (neglecting the intercept). At pH 4, this procedure introduced an error of ca. 20%, which was smaller at higher pHs.

Some complementary experiments using either substoichiometric or a small excess of cysteine were done using the diode array spectrophotometer and the rapid kinetics accessory described above. The concentration ranges of the complex and cysteine were $(0.7-1.5) \times 10^{-4}$ M and $(0.17-1.5) \times 10^{-4}$ M, respectively. The experiments were done at pH 4.0 (0.1 M acetate buffer), $I = 1$ M, NaCl.

Results and Discussion

For the selection of the reaction conditions, we considered the most significant work on the adduct-formation reactions of NP with thiols,[10a,b] comprising the pH range 8−10, that is, with the thiols (nearly) fully deprotonated [pK_a(RSH) = ∼8]. Under these pH conditions, $[Fe(CN)_5NO]^{3-}$ is the predominant species arising as a product of the reaction of NP with the thiols, with minor quantities of $[Fe(CN)_4NO]^{2-}$ in a fast equilibrium.[4,7,11a] The upper limit of 10 is appropriate for avoiding the competitive attack of OH^-.[3] A fast equilibrium is settled in the formation process of the red adduct, eq 1. For a broad range of studied thiols, the absorption

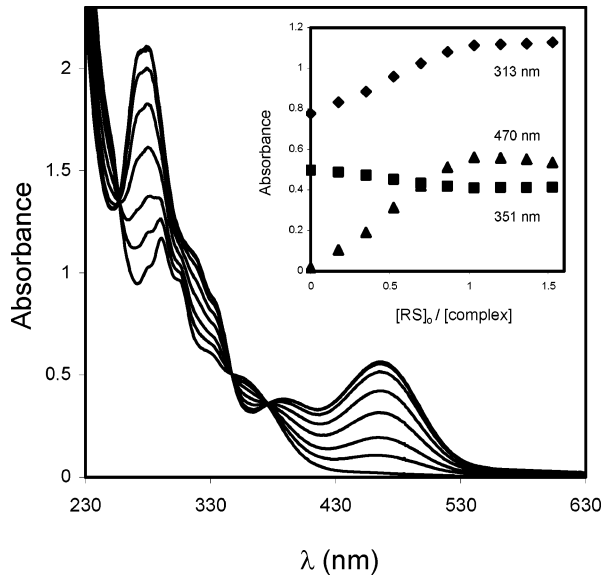

Figure 1. Successive spectra recorded during the addition of 0.1 mL aliquots of a 2.02×10^{-3} M cysteine solution to 20 mL of a 5.71×10^{-5} M solution of $[Ru(bpy)NO(tpy)]^{3+}$. pH 4.0 (0.1 M acetate buffer), $I = 1$ M (NaCl), $T = 25$ °C. $[RS]_o$ is the analytical concentration of cysteine.

maxima lay at ca. 520 nm, with $\epsilon = \sim(5-10) \times 10^3$ M^{-1} cm^{-1}.[8,9] Both the adduct-formation and dissociation rate constants have been determined ($I = 0.4$ M, 25 °C). For L-cysteine, $k_1 = 2.2 \times 10^4$ $M^{-1}s^{-1}$ and $k_{-1} = 3.4 \times 10^2$ s^{-1}, at pH 10.0.[8]

$$[Fe(CN)_5NO]^{2-} + RS^- \rightleftarrows [Fe(CN)_5N(O)SR]^{3-} \qquad k_{1(RS^-)},\ k_{-1(RS^-)} \quad (1)$$

Reaction 1 was studied with T-jump techniques, because the fast reactions of NP with thiolates are in the detection limit of the SF procedure.[8] In the present work, we were able to reproduce the values for both rate constants in reaction 1 even under these extreme SF conditions. However, the reactions of the ruthenium nitrosyl complexes with cysteine appeared to be very fast at pH 10. As the deprotonated thiols, RS^-, are the only active species in the nucleophilic process (systematic experiments as a function of pH showed that the RSH species were unreactive,[8] see below), we could afford the SF kinetic studies by decreasing the pH, thus controlling the effective concentration of RS^-. Most of the work was performed under an excess of cysteine over the ruthenium complex. This situation is seemingly the one present in bodily fluids containing a high concentration of reduced sulfur species in vivo.[5b]

The results will be ordered according to the different time scales for the events occurring after mixing. First, we address the reactions for cysteine adding to the different nitrosyl complexes, as detailed in Table 1. Second, we consider the decay of these adducts, as observed in the UV−vis spectral runs, giving additional intermediates in the route to final products.

Formation and Dissociation Reactions of the First Intermediate, I_1. Figure 1 shows the spectra obtained after the addition of aliquots of a solution of cysteine to a solution of $[Ru(bpy)NO(tpy)]^{3+}$. A new band centered at 467 nm, a shoulder at 390 nm, and other new bands below 340 nm can be appreciated. The isosbestic points at 347 and 376 nm are evidence of a clean reaction. The spectra remain constant after the addition of 0.95 equiv of cysteine (see inset, Figure 1), sustaining a 1:1 stoichiometry. Upon addition of larger amounts of cysteine, new spectral changes were observed as a result of further reactivity (see below). We describe the product of the primary interaction as the adduct intermediate $\mathbf{I_1}$, similar to the one described in eq 1. The intense bands obtained upon the addition of cysteine to NP and to the presently reported complexes can be traced to metal-to-ligand charge transfer (MLCT) transitions in the $\{(X)_5MN(O)SR\}$ adducts, which are expectedly shifted to the blue for the ruthenium-based adducts compared to those for the NP−thiolate adducts.[13]

A similarity in the electronic structures of the $\{(X)_5MN(O)L\}$ adducts (L = nucleophile) can be proposed on the basis of the following experimental and theoretical evidence. In a general way, the addition processes involve a change in geometry, from a linear $\{(X)_5M(NO^+)\}$ to an angular $\{(X)_5MN(O)L)\}$ moiety.[2] The reactions can be described by a change in N hybridization from sp to sp^2 or, alternatively, as a conversion from a $\{MNO\}^6$ to a $\{MNO\}^8$ species,[2b] as a result of the location of the electron pair of the nucleophile in the vacant LUMO of the reactant. Evidence for this linear-to-bent conversion comes from the solid structure of $[Ru(bpy)_2ClN(O)SO_3]$,[14] in which the angular RuN(O)S moiety is clearly identified, and also by the DFT calculations regarding the reaction progress of NP with OH^-, leading to the nitrous acid bound intermediate.[6] The conversion also involves the triple bond in the NO^+ reactant becoming a double NO bond in the $\{(X)_5MN(O)L\}$ moieties. This has been nicely demonstrated through the IR measurements in the reaction of NP with EtS^-, showing the appearance of a peak at 1380 cm^{-1} as characteristic of the red adduct.[15] All of this evidence points to the existence of common general features in the geometry and electronic structure of the $\{(X)_5MN(O)L\}$ adducts, even if we change the metal, the coligands (X), or the nucleophiles (L).

A similar experiment was performed with the *cis*-$[Ru(bpy)_2ClNO]^{2+}$ complex, and a new band at 450 nm with a shoulder at 410 nm was observed. A 3-fold excess of cysteine over the complex concentration had to be added in order to reach a maximum conversion. This is consistent with the establishment of an equilibrium reaction, similar to the one described in eq 1.

(13) We tried to obtain confirmative evidence on the structure of the $\mathbf{I_1}$ adduct. As shown in ref 15, a distinctive IR absorption should be expected in the 1400 cm^{-1} region for the N=O stretching in the nitrosothiolate ligand. Unfortunately, intense C−H absorptions from the polypyridine ligands precluded any clear assignments coming from IR or Raman spectra. Besides, only indirect evidence could be obtained with field-desorption mass spectrometry measurements. Thus, the observed spectra for the mixtures of the nitrosyl complex with cysteine showed evidence of thermal dissociation of the nitrosothiolate ligand, through the appearance of peaks at 596 and 716 au, which may be assigned to $[Ru(bpy)_2Cl(PF_6)]$ and $[Ru(bpy)_2Cl(PF_6)(cys)]$ substitution products.

(14) Bottomley, F.; Brooks, W. V. F.; Paez, D. E.; White, P. S.; Mukaida, M. *J. Chem. Soc., Dalton Trans.* **1983**, 2465.

(15) Schwane, J. D.; Ashby, M. T. *J. Am. Chem. Soc.* **2002**, *124*, 6822−6823.

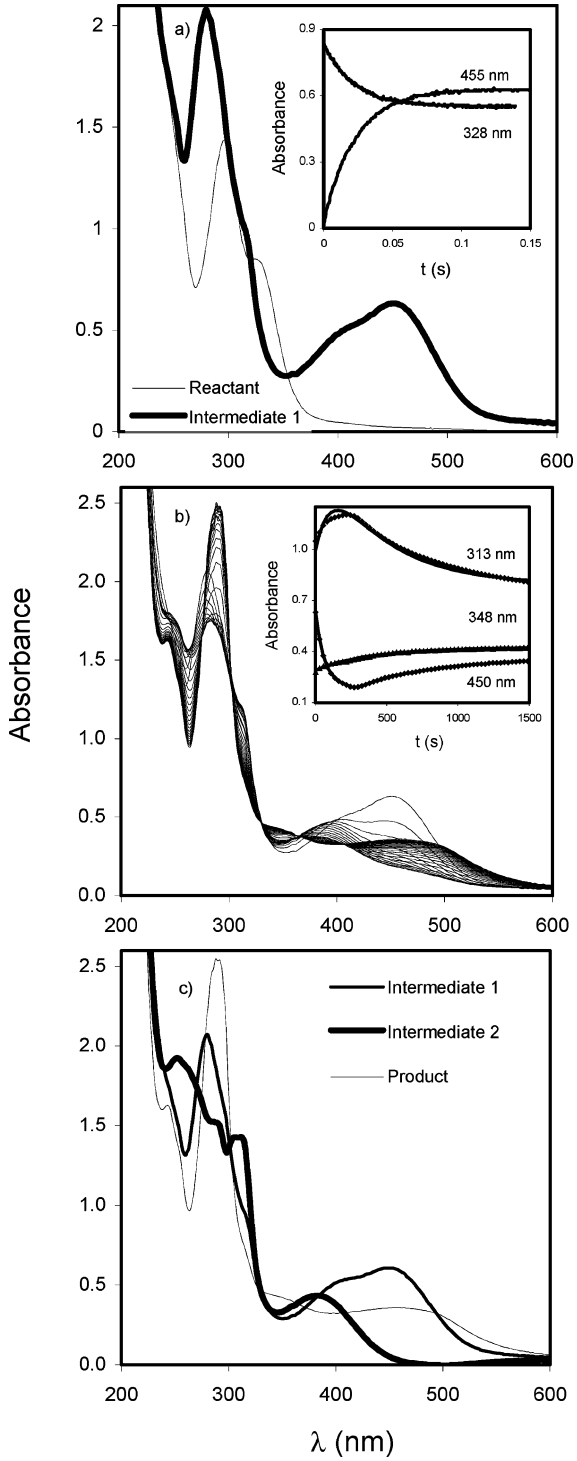

Figure 2. UV−vis spectral changes for the reaction of $[Ru(bpy)_2ClNO]^{2+}$ with cysteine. [Complex] = 8.1×10^{-5} M, [cysteine] = 3.8×10^{-3} M, pH 4.0 (0.1 M acetic buffer), $I = 1$ M (NaCl), $T = 25.0$ °C. (a) UV−vis spectra of $[Ru(bpy)_2ClNO]^{2+}$ without and after the addition of cysteine (reactant and $\mathbf{I_1}$, respectively). Inset: kinetic traces at 455 and 328 nm corresponding to the formation of $\mathbf{I_1}$, $k_{1obs} = 43\ s^{-1}$. (b) Successive spectra corresponding to the decomposition of $\mathbf{I_1}$ to produce $\mathbf{I_2}$ and the product. $k_{2obs} = 1.0 \times 10^{-2}\ s^{-1}$ and $k_{3obs} = 3 \times 10^{-3}\ s^{-1}$. Inset: kinetic traces at different wavelengths. (c) Spectra of the product, and of $\mathbf{I_1}$ and $\mathbf{I_2}$, obtained through a SPECFIT analysis of the results shown in part b.

Figure 2 shows the spectral changes for the reaction of *cis*-$[Ru(bpy)_2ClNO]^{2+}$ with an excess of cysteine. Figure 2a shows the spectrum of the intermediate formed in the first reaction step, which is consistent with the bands observed

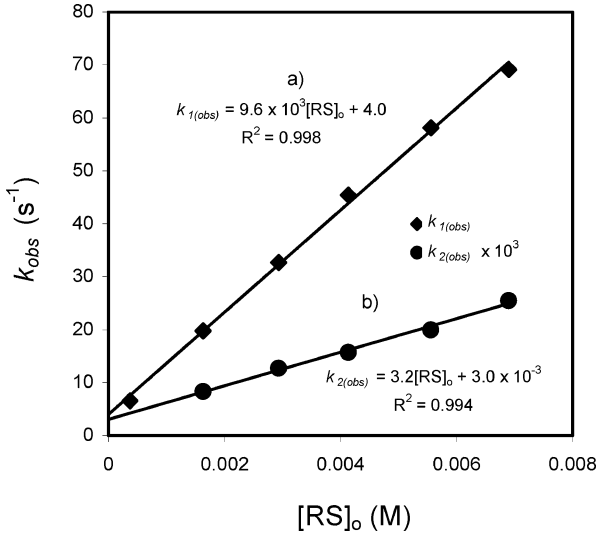

Figure 3. Cysteine-concentration dependence of the observed rate constant for the first (k_{1obs}) and second (k_{2obs}) reaction steps for the *cis*-$[Ru(bpy)_2ClNO]^{2+}$ complex. $T = 25.0$ °C, pH 4.0 (0.1 M acetate buffet), $I = 1$ M (NaCl). k_{2obs} values were multiplied by 10^3 to fit the scale.

during the titration (*vide supra*). By measuring at different wavelengths, we obtained the same values of k_{obs}. From here on, we describe the first formed adducts of cysteine with all of the Ru complexes as $\mathbf{I_1}$.

Figure 3a shows the cysteine-concentration dependence of k_{1obs} for the formation of $\mathbf{I_1}$, for the *cis*-$[Ru(bpy)_2ClNO]^{2+}$ complex. A linear distribution appears, with a slope that can be traced to k_1 and an appreciable intercept assignable to k_{-1}. To assign these rate constants, we must consider the acid−base equilibrium of cysteine, eq 2, and the reactions of RS^- and RSH with the nitrosyl complex (reactions 3 and 4).[8] In this way, we obtain eqs 5 and 6, where k_1 is the second-order rate constant for the first step ($i = 1$) and k_{-1} is the intercept corresponding to the plots of k_{obs} versus $[RS]_o$ (analytical concentration of cysteine).

$$RSH \rightleftarrows RS^- + H^+ \qquad K_a \tag{2}$$

From the literature, pK_a is 8.3 for cysteine.[16] According

$$[(X)_5RuNO]^n + RS^- \rightleftarrows [(X)_5RuN(O)SR]^{n-1} \qquad k_{1(RS^-)},\ k_{-1(RS^-)} \tag{3}$$

$$[(X)_5RuNO]^n + RSH \rightleftarrows [(X)_5RuN(O)SR]^{n-1} + H^+ \qquad k_{1(RSH)},\ k_{-1(RSH)} \tag{4}$$

$$k_i = \frac{k_{i(RS^-)}K_a + k_{i(RSH)}[H^+]}{K_a + [H^+]} \tag{5}$$

$$k_{-i} = k_{-i(RS^-)} + k_{-i(RSH)}[H^+] \tag{6}$$

to eq 5, when $[H^+] \gg K_a$, a plot of the second-order rate constant k_1 versus $1/[H^+]$ should be linear, with a slope equal to $k_{1(RS^-)}K_a$ and an intercept equal to $k_{1(RSH)}$. Figure 4a shows this plot for the first reaction step. A linear distribution is

(16) *CRC Handbook of Chemistry & Physics*, 75th ed.; Frederikse, H. P. R., Lide, D. R., Eds.; CRC Press: Boca Raton, FL, 1994.

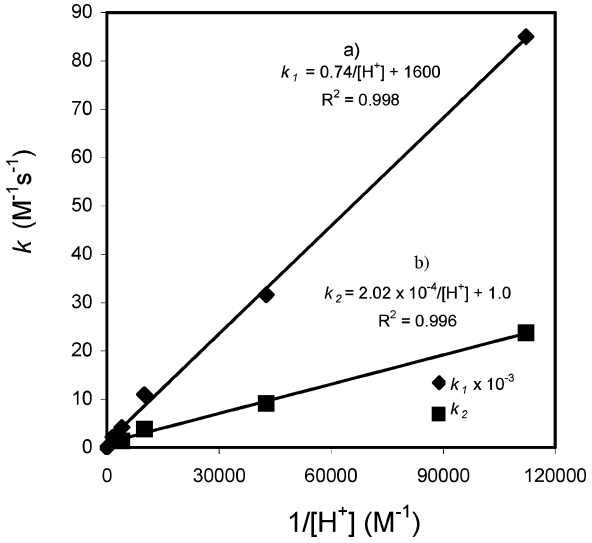

Figure 4. Plot of the second-order rate constant for the first (k_1) and second (k_2) reaction steps vs 1/[H^+] for the *cis*-[Ru(bpy)$_2$ClNO]$^{2+}$ complex. T = 25.0 °C, pH 3.2−5.0 (0.1 M acetate buffer), I = 1 M (NaCl), [Ru(bpy)$_2$ClNO^{2+}] = 9 × 10^{-5} M, [RS]$_o$ = 8.2 × 10^{-3} M. k_1 values were multiplied by 10^{-3} to fit the scale.

observed with no meaningful intercept. This means that $k_{1(RSH)}$ is negligible in our reaction conditions.

The spectral changes during the reactions of cysteine with the rest of the complexes of Table 1 were similar to those observed with the *cis*-[Ru(bpy)$_2$ClNO]$^{2+}$ complex in Figure 2. The bands for $\mathbf{I_1}$ were observed in the range 405−470 nm. In all cases, the formation of $\mathbf{I_1}$ was studied as a function of the concentration of cysteine. The reactions always showed a linear distribution, with appreciable intercepts in most cases, thus affording values for k_{-1}. The values of the rate constants are included in Table 2. The values obtained for k_1 cannot be compared, because they have been measured at different pHs. Considering that only the deprotonated form of cysteine is reactive, we calculate $k_{1(RS^-)}$ for the different complexes using eq 5 (see Table 2).

Figure 5 shows a plot of ln $k_{1(RS^-)}$ versus $E_{NO+/NO}$ (redox potential of the coordinated nitrosyl). A linear correlation is observed in the lower potential range, that is, for the least reactive complexes. The most reactive ones show values of $k_{1(RS^-)}$ close to the diffusion limit of 10^9 M^{-1} s^{-1}. Recently obtained values corresponding to the addition of OH^- to the same complexes[6] are also shown in Table 2 and Figure 5 for comparative purposes. The rate constants for the additions of thiolates, RS^-, are expectedly greater than those for OH^-, given the greater relative nucleophilic ability of sulfur. However, it can be seen that the values of the slopes are similar, close to 20 V^{-1}, for the lines corresponding to the reactions with OH^- and the meaningful values for the reactions with RS^-.

The significance of this linear free energy relationship (LFER) has been analyzed recently for the adduct formation reactions in which the linear {(X)$_5$M(NO^+)} moieties are transformed into the angular {(X)$_5$MN(O)OH} ones in the respective addition processes.[6] The increase in the rates for the complexes with more positive reduction potentials was shown to be related to an increase in the positive charge at the electrophilic MNO moiety. Interestingly, the activation parameters indicated that the rate increase was associated with an activation enthalpy *increase*, overcompensated by the large activation entropies displayed by the positively charged complexes when reacting with OH^-. Given the similar slopes in Figure 5, we can reasonably assume an analogous mechanism for the additions of RS^- nucleophiles as well.

The Decay of the Adduct Intermediate $\mathbf{I_1}$, with Formation of Intermediate $\mathbf{I_2}$. For [Ru(bpy)$_2$ClNO]$^{2+}$, $\mathbf{I_1}$ reacts in a second reaction step to produce a second intermediate, $\mathbf{I_2}$, which shows a well-defined band centered at 384 nm (Figure 2b, Table 1). Figure 3b shows the plot of k_{obs} against the concentration of cysteine for this second reaction step, showing a behavior similar to the one found for the first step. Thus, k_2 and k_{-2} can be obtained from the slope and intercept, respectively. We propose that $\mathbf{I_2}$ contains two coordinated, deprotonated cysteines, eq 7.

$$[(X)_5RuN(O)SR]^{n-1} + RS^- \rightleftarrows [(X)_5RuN(O)(SR)_2]^{n-2} \qquad k_{2(RS^-)},\ k_{-2(RS^-)} \quad (7)$$

This type of intermediate has been proposed in the reaction of NP with an excess of thiolate.[10a] No direct spectroscopic evidence was provided, but a linear dependence of the pseudo-first-order rate constant for the decay of [(NC)$_5$FeN(O)SR]$^{3-}$ on the concentration of cysteine was reported,[10a,b] as described here. Also, similar structures comprising two thiolates bound to the N atom of NO have been proposed during the transnitrosation reactions of thiols,[17a,b] and recent NMR results together with DFT calculations provide evidence for these elusive intermediates.[17c] In Figure 4b, the linear plot of the second-order rate constant, k_2, against the inverse of [H^+] shows, again, that reaction 8 involving the protonated cysteine, RSH, can be neglected, as found for the formation of $\mathbf{I_1}$ (eq 4).

$$[(X)_5RuN(O)SR]^{n-1} + RSH \rightleftarrows [(X)_5RuN(O)(SR)_2]^{n-2} + H^+ \qquad k_{2(RSH)},\ k_{-2(RSH)} \quad (8)$$

Figure 5 shows a linear behavior in the plots of ln $k_{2(RS^-)}$ for the second step in eq 7 against the redox potential, for the same series of ruthenium complexes (again, k_2 was corrected for the pH effect using eq 6, i = 2). The alignment of the points together with the ones for the OH^- additions is fortuitous. However, it is entirely reasonable that the rates for the addition of an RS^- nucleophile in reaction 7 must be lower than those in reaction 3, because the first bound thiolate has already diminished the nucleophilic ability of the MNO group. Overall, the plots in Figure 5 provide consistent evidence of the successive RS^- additions on the nitrosyl complexes, as described by eqs 3 and 7.

(17) (a) Dicks, A.; Li, E.; Munro, A.; Swift, H.; Williams, D. *Can. J. Chem.* **1998**, *76*, 789−794. (b) Houk, K. N.; Hietbrink, B. N.; Bartberger, M. D.; McCarren, P. R.; Choi, B. Y.; Voyksner, R. D.; Stamler, J. S.; Toone, E. J. *J. Am. Chem. Soc.* **2003**, *125*, 6972−6976. (c) Perissinotti, L. L.; Turjanski, A. G.; Estrín, D. A.; Doctorovich, F. *J. Am. Chem. Soc.* **2005**, *127*, 486−487.

Table 2. Kinetic Results for the Reactions of Cysteine with Different Nitrosyl Complexes[a]

complex	$10^{-4}\,k_1$ ($M^{-1}s^{-1}$)	k_{-1} (s^{-1})	k_2 ($M^{-1}s^{-1}$)	$10^2\,k_{-2}$ (s^{-1})
1: $[Fe(CN)_5NO]^{2-}$	2.2 ± 0.4[b]	560 ± 20[b]	$1-2$[c]	
2: $[Ru(edta)NO]^{-}$	4.9 ± 0.6[b]	260 ± 20[b]	~ 50[b]	
3: *trans*-$[Ru(NH_3)_4NO(pz)]^{3+}$	16 ± 3[d]	110 ± 40[d]	60 ± 4[d]	2.8 ± 0.6[d]
4: *cis*-$[Ru(bpy)_2ClNO]^{2+}$	0.96 ± 0.02	4.0 ± 0.9	3.2 ± 0.1	0.3 ± 0.07
5: *cis*-$[Ru(bpy)_2(NO_2)NO]^{2+}$	1.36 ± 0.03	2 ± 1	11.6 ± 0.2	0.29 ± 0.09
6: *trans*-$[NCRu(py)_4CNRu(py)_4NO]^{3+}$	0.70 ± 0.01	1.5 ± 0.3	35 ± 1	1.9 ± 0.5
7: $[Ru(bpy)NO(tpy)]^{3+}$	2.67 ± 0.08	<3	35 ± 2	<0.9
8: *cis*-$[Ru(AcN)(bpy)_2NO]^{2+}$	2.89 ± 0.07	4 ± 2	18 ± 4	9 ± 1
9: $[Ru(bpz)NO(tpy)]^{3+}$	3.56 ± 0.08	<5	179 ± 4	<3

complex	$k_{1(RS^-)}$ ($M^{-1}s^{-1}$)[e]	$k_{2(RS^-)}$ ($M^{-1}s^{-1}$)[e]	k_{OH} ($M^{-1}s^{-1}$)[f]	E_{NO^+/NO° (v)[f]
1: $[Fe(CN)_5NO]^{2-}$	2.2×10^4	$1-2$[c]	0.55	-0.29
2: $[Ru(edta)NO]^{-}$	4.9×10^4	~ 50	4.35	-0.30
3: *trans*-$[Ru(NH_3)_4NO(pz)]^{3+}$	3.2×10^6	1.2×10^3	1.77×10^2	-0.11
4: *cis*-$[Ru(bpy)_2ClNO]^{2+}$	1.5×10^8	4.0×10^4	8.5×10^3	0.05
5: *cis*-$[Ru(bpy)_2(NO_2)NO]^{2+}$	2.7×10^8	2.3×10^5	5.06×10^4	0.18
6: *trans*-$[NCRu(py)_4CNRu(py)_4NO]^{3+}$	1.4×10^8	7.0×10^5	9.2×10^3	0.22
7: $[Ru(bpy)NO(tpy)]^{3+}$	5.3×10^8	7.0×10^5	3.17×10^5	0.25
8: *cis*-$[Ru(AcN)(bpy)_2NO]^{2+}$	5.8×10^8	3.6×10^5	5.60×10^6	0.35
9: $[Ru(bpz)NO(tpy)]^{3+}$	7.1×10^8	3.6×10^6	7.6×10^6[g]	0.46[g]

[a] pH 4.0 (0.1 M acetate buffer), $I = 1$ M (NaCl), $T = 25.0$ °C, unless otherwise stated. [b] pH 9.9 (0.1 M borate buffer), $I = 1$ M (NaCl). [c] From ref 10a,b. [d] pH 7.0 (0.1 M phosphate buffer), $I = 1$ M (NaCl). [e] Calculated from eq 5, using $pK_a = 8.3$. [f] From ref 6. [g] This work ($I = 1$ M NaCl, $T = 25.0$ °C).

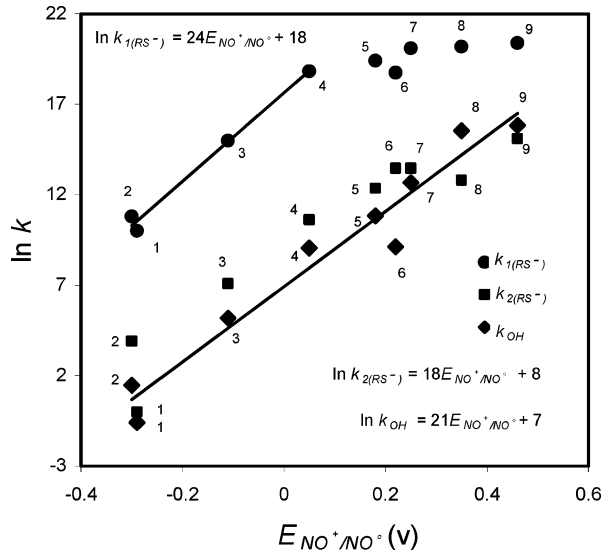

Figure 5. Linear free energy relationships (LFER) for $k_{1(RS^-)}$, $k_{2(RS^-)}$, and k_{OH}. For number assignments, see Tables 1 or 2.

In our experiments with substoichiometric cysteine, we also observed the formation and decay of the $\mathbf{I_1}$ absorptions, with rate constants in the range 3×10^{-3} s^{-1} to 4×10^{-4} s^{-1}. No one-electron reduction products could be found for the ruthenium complexes **4**, **5**, **7**, and **8** (Table 1), given that $[Fe(CN)_5NO]^{3-}$ was confirmed by us as the product in the reaction of NP with cysteine.[10a,c] (The redox decay of $[(NC)_5FeN(O)SR]^{3-}$ led to identical products, $[Fe(CN)_5NO]^{3-}$ and cystine, under working conditions of either substoichiometric or excess cysteine.)[10a] For complex **4**, no IR absorptions were found in the range 1600−1800 cm^{-1}, as expected for reduced nitrosyl.[7] A very weak EPR signal at ca. 3400 G was measured, which cannot be assigned to the NO-bound complex. The UV−vis absorption spectra of the products indicate the presence of the Ru−aqua ions. This suggests that a two-electron nitrosyl reduction could also be operative, as described below under conditions of excess cysteine.[18]

The Decay of Intermediate $\mathbf{I_2}$. N_2O vs NO as Reduction Products. Figure 2b shows that $\mathbf{I_2}$ decomposes slowly (third reaction step, k_3) to a product with bands centered at 470 and 350 nm. Figure 2c shows the spectra corresponding to both intermediates, $\mathbf{I_1}$ and $\mathbf{I_2}$, together with the one for the final product, as obtained through a SPECFIT analysis.[19] Further reactions of the product were not investigated in detail. Its spectrum closely resembles that of the *cis*-$[Ru(bpy)_2Cl(H_2O)]^+$ ion.[20] Moreover, a new wave at 0.49 V versus Ag/AgCl was observed during this reaction by performing the SWV experiments. A wave in the same position appeared after the reduction of *cis*-$[Ru(bpy)_2ClNO]^{2+}$ at −1.0 V versus Ag/AgCl. It is well-known that the last procedure generates the $[Ru(bpy)_2Cl(H_2O)]^+$ complex in a clean way, consistent with the *two-electron reduction* process occurring at the stated potential.[20]

During this third reaction step, N_2O was produced, as detected by IR spectroscopy through its characteristic band at 2230 cm^{-1}.[10e] We propose reaction 9 for describing the decomposition of $\mathbf{I_2}$ starting with the *cis*-$[Ru(bpy)_2ClNO]^{2+}$ complex, and we assume that similar processes are also operative for the other Ru complexes.

$$cis\text{-}[Ru(bpy)_2ClN(O)(SR)_2] + H^+ \rightleftarrows cis\text{-}[Ru(bpy)_2Cl(HNO)]^+ + RS{-}SR \quad (9)$$

Equation 9 describes a two-electron reduction of NO^+, giving the labile nitroxyl ligand, HNO. A subsequent fast coupling process leads to N_2O, eq 10, as described elsewhere.[21]

$$2HNO \rightarrow N_2O + H_2O \quad (10)$$

Evidence of the lability of HNO in the ruthenium complexes is provided by the irreversibility of the two-electron reduction

(18) An intermediate character can be envisaged for the less reactive Ru complexes **2** and **3**. In the reaction of $[Ru(NH_3)_4NOpz]^{3+}$ with cysteine, a new absorption at ca. 1800 cm^{-1} developed, which could probably be ascribed to a one-electron reduction process.

(19) Binstead, R. A.; Zuberbülher, A. D. *SPECFIT*; Spectrum Software Associates: Chapel Hill, NC, 1993−1999.

(20) Togniolo, V.; Santana da Silva, R.; Tedesco, A. C. *Inorg. Chim. Acta* **2001**, *316*, 7−12.

Scheme 1

$$[(X)_5RuNO]^n \underset{-RS^-}{\overset{RS^-}{\rightleftharpoons}} [(X)_5RuN(O)SR]^{n-1} \underset{-RS^-}{\overset{RS^-}{\rightleftharpoons}} [(X)_5RuN(O)(SR)_2]^{n-2} \longrightarrow [(X)_5Ru(H_2O)]^{n-1} + \tfrac{1}{2}N_2O + RSSR$$

waves in the electrochemical experiments.[12b] We observed a white precipitate of cystine in the aged solutions, in the experiments with the most concentrated solutions, as found previously by other authors.[10]

The reason for the different behavior of NP compared to the ruthenium complexes may be traced to the different reactivity of the corresponding adducts toward *redox decomposition*, implying a different nature for the products with either NP or the Ru complexes. The nitrosyl group in NP has a comparatively low redox potential (Table 2), but it can be easily reduced by one electron, leading to $[Fe(CN)_5NO]^{3-}$; this is obtained after decomposition of the $\mathbf{I_1}$ adduct, through the homolytic cleavage of the N−S bond.[3] Remarkably, the same product is obtained with a high excess of cysteine, where some $\mathbf{I_2}$ adduct is also expected to be present (the rates of $\mathbf{I_2}$ formation are comparatively low for NP, cf. the $k_{2(RS^-)}$ values in Table 2). It is probable that the two-electron reduction is not thermodynamically allowed in $\mathbf{I_2}$. In this context, we should address the fact that N_2O has been detected through IR spectroscopy at delayed times after mixing NP with excess glutathione, ascorbate, or NADH in the hours time scale (pH 7.2).[10e] We believe that N_2O is not generated through a direct two-electron reduction at bound NO^+, but through a novel mechanistic route comprising the disproportionation reactivity of dinitrosyl intermediates. We rely on the recently reported evidence in a study of the thermal decomposition of reduced NP (pH range 4−10).[11a]

In contrast to NP, the Ru complexes afford a fast conversion of $\mathbf{I_1}$ to $\mathbf{I_2}$, avoiding the previously described one-electron route, and lead to N_2O through a two-electron reduction. This also seems to occur under conditions of substoichiometric cysteine (see above). Thus, kinetic as well as thermodynamic factors appear to control the formation of N_2O against NO for the more oxidizing ruthenium nitrosyl complexes, influencing the decomposition of $\mathbf{I_2}$, which has an appropriate configuration favoring a two-electron transfer.

The influence of the structure of the nucleophile in the one-electron or multielectronic reductions of bound NO^+ in NP has been recently discussed by using hydrazine and substituted hydrazines as nucleophiles. HNO-bound intermediates have been proposed in some of these systems as precursors of N_2O.[22] On the other hand, the present work deals with the changes produced by $\{X_5M(NO^+)\}$ moieties with different oxidizing capabilities, for a given nucleophile.

Summary and Conclusions

The nucleophilic addition reactions under an excess of cysteine have been studied for a number of ruthenium nitrosyl complexes. The reactions are very fast, compared to previously reported additions of OH^- and N-binding nucleophiles. The primary interaction of cysteine with the complexes generates 1:1 adduct intermediates, $\mathbf{I_1}$, with intense absorption bands in the range 410−470 nm, assigned to MLCT transitions, structurally related to the similar adduct with NP absorbing at 526 nm. The formation reactions are first order in each of the reactants, whereas the dissociations are first order in the adduct.

The bands of $\mathbf{I_1}$ decay in an excess of cysteine, and a second intermediate, $\mathbf{I_2}$, is produced, with intense absorption bands between 340 and 400 nm. The formation rates are slower for $\mathbf{I_2}$ than for $\mathbf{I_1}$, but the kinetic order in the formation and dissociation reactions of both intermediates were the same. We propose that $\mathbf{I_2}$ is another adduct, with a 2:1 stoichiometry (thiolate vs nitrosyl complex). Additional evidence of these successive adduct-formation reactions is provided by the linear free energy plots of the addition-rate constants against the reduction potentials of the NO^+/NO couples. As in the reactions of OH^- with a set of nitrosyl complexes, the addition of thiolates is faster for the complexes affording more positive reduction potentials.

$\mathbf{I_2}$ decays further with the formation of the corresponding aqua complexes, $\{(X)_5Ru(H_2O)\}$, N_2O, and cystine. Negative evidence was obtained (IR, EPR) for $[Ru(bpy)_2Cl(NO)]^+$ as to the presence of bound NO radicals, in contrast with NP. Instead, the observed products account for a two-electron reduction of the initial NO^+-bound species, favored by the structures of the $\mathbf{I_2}$ adducts containing two thiolates and by the oxidizing ability of the nitrosyl moieties. In contrast, the less oxidizing NP adducts ($\mathbf{I_1}$, and the poorly stable $\mathbf{I_2}$) always decompose through a one-electron process. Scheme 1 summarizes our proposed mechanism for the ruthenium complexes.

Given the one-electron vs two-electron nitrosyl-reduction products for NP and the ruthenium complexes, respectively, a final comment is in order on the connection of these mechanistic issues with the role of thiolates on the release of NO to the medium when NP is injected, a crucial point for triggering the vasodilation process. We have recently shown that bound NO is very inert toward dissociation when we consider it as predominantly $[Fe(CN)_5NO]^{3-}$ (at pHs greater than 8) or as $[Fe(CN)_4NO]^{2-}$ (at lower pHs).[11a] Therefore, the role of thiolates should be ascribed, in principle, to the ability of reducing NO^+ to NO, still as a bound species, with no other influence favoring the mobilization of NO to the enzymatic targets. Intracellular conditions appropriate to first favoring the prior release of cyanides should be needed for NO labilization from reduced NP, thus accounting for the fast response (minute time scale) upon injection into the bodily fluids.[4,11a] We comment separately[23] on an alternative possibility of free NO generation from NP

(21) (a) Bonner, F. T.; Stedman, G. In *Methods in Nitric Oxide Research*; Feelisch, M., Stamler, J. S., Eds.; Wiley: Chichester, U. K., 1996; Chapter 1. (b) Shafirovich, V.; Lymar, S. V. *Proc. Natl. Acad. Sci. U.S.A.* **2002**, *99*, 7340−7345.

(22) Gutiérrez, M. M.; Amorebieta, V. T.; Estiú, G. L.; Olabe, J.-A. *J. Am. Chem. Soc.* **2002**, *124*, 10307−10319.

in the presence of thiolates, starting with the dissociation of the N(O)SR ligand. This could hardly be sustainable for the presently reported ruthenium nitrosyl complexes because of the presence of much more inert Ru−N bonds, precluding a fast N(O)SR dissociation from the $\{(X)_5RuN(O)SR\}$ adducts.

(23) The intramolecular decomposition of the NP−cysteine adduct $\mathbf{I_1}$, $\{(NC)_5FeN(O)SR\}^{3-}$, giving $[Fe(CN)_5NO]^{3-}$ and the thiyl radical, occurs with a rate constant of ca. 10^{-3} to 10^{-4} s^{-1}.[10] We estimate a similar rate for the dissociation of the nitrosothiolate ligand, N(O)-SR, through the cleavage of the M−N bond, by comparing with data for the pentacyano(L)ferrate(II) complexes.[24] If the latter process is operative, we predict that NO may appear in the solutions through the well-known homolytic decomposition of free N(O)SR.[25] Although NO could recombine with $[Fe(CN)_5H_2O]^{3-}$ ($k = 250$ M^{-1} s^{-1}, 25.4 °C),[26] the presence of sGC in the medium would compete successfully for NO trapping ($k = \sim 10^8$ M^{-1} s^{-1}),[27] leading to vasodilation. Our qualitative experiments with the NP−cysteine adduct in the presence of pyrazine (pz), reveal the formation of both $[Fe(CN)_5NO]^{3-}$ and some $[Fe(CN)_5pz]^{3-}$, suggesting that both N(O)SR dissociation and homolytic scission of the N−S bond in $\{(NC)_5FeN(O)SR\}^{3-}$ occur on comparable time scales.

Acknowledgment. This work was supported by the University of Buenos Aires and by the Government Agencies ANPCYT and CONICET. F.R. and J.A.O. are a graduate fellow and a member of the scientific staff of CONICET, respectively. We thank Professor Douglas W. Franco for providing us solid samples of complexes **2** and **3**, and to Professors Valentín Amorebieta and Luis Perissinotti for the EPR measurements.

IC048156D

(24) Baraldo, L. M.; Forlano, P.; Parise, A. R.; Slep, L. D.; Olabe, J. A. *Coord. Chem. Rev.* **2001**, *219−221*, 881−921.
(25) (a) Stamler, J. S.; Toone, E. J. *Curr. Opin. Chem. Biol.* **2002**, *6*, 779−785. (b) Szacilowski, K.; Stasicka, Z. *Prog. React. Kinet.* **2000**, *26*, 1−58.
(26) Roncaroli, F.; Olabe, J. A.; van Eldik, R. *Inorg. Chem.* **2003**, *42*, 4179−4189.
(27) Ballou, D. P.; Zhao, Y.; Brandish, P. E.; Marletta, M. A. *Proc. Natl. Acad. Sci. U.S.A.* **2002**, *99*, 12097−12101.